Reciprocated Suppression of Polymer Crystallization Toward Improved Solid Polymer Electrolytes: Higher Ion Conductivity and Tunable Mechanical Properties

Sheng Bi,[1] Che-Nan Sun,[2] Thomas A. Zawodzinski Jr.,[2,3] Fei Ren,[4] Jong Kahk Keum,[5,6] Suk-Kyun Ahn,[6,7] Dawen Li,[1] Jihua Chen[6]

[1]Department of Electrical and Computer Engineering Center for Materials Information Technology, University of Alabama, Tuscaloosa, Alabama 35487

[2]Materials Science & Technology Division, Oak Ridge National Laboratory, P.O. Box 2008, Oak Ridge, Tennessee

[3]Department of Chemical and Biomolecular Engineering, University of Tennessee, Knoxville, Tennessee 37996

[4]Department of Mechanical Engineering, Temple University, Philadelphia, Pennsylvania 19122

[5]Neutron Scattering Science Division, Oak Ridge National Laboratory, Oak Ridge, Tennessee 37831

[6]Center for Nanophase Materials Sciences, Oak Ridge National Laboratory, Oak Ridge, Tennessee 37831

[7]Department of Polymer Science and Engineering, Pusan National University, Busan, Republic of Korea, 609-735

Correspondence to: J. Chen (E-mail: chenj1@ornl.gov) or D. Li (E-mail: dawenl@eng.ua.edu)

ABSTRACT: Solid polymer electrolytes based on lithium bis(trifluoromethanesulfonyl) imide and polymer matrix were extensively studied in the past due to their excellent potential in a broad range of energy related applications. Poly(vinylidene fluoride) (PVDF) and polyethylene oxide (PEO) are among the most examined polymer candidates as solid polymer electrolyte matrix. In this work, we study the effect of reciprocated suppression of polymer crystallization in PVDF/PEO binary matrix on ion transport and mechanical properties of the resultant solid polymer electrolytes. With electron and X-ray diffractions as well as energy filtered transmission electron microscopy, we identify and examine the appropriate blending composition that is responsible for the diminishment of both PVDF and PEO crystallites. A three-fold conductivity enhancement is achieved along with a highly tunable elastic modulus ranging from 20 to 200 MPa, which is expected to contribute toward future designs of solid polymer electrolytes with high room-temperature ion conductivities and mechanical flexibility. © 2015 Wiley Periodicals, Inc. J. Polym. Sci., Part B: Polym. Phys. **2015**, *53*, 1450–1457

KEYWORDS: blends; crystallization; ion conductivity; polymer crystallization; reciprocated suppression; solid polymer electrolytes; TEM

INTRODUCTION The solid polymer electrolyte (SPE) has attracted wide attentions in the pursuit toward next-generation capacitors and batteries, due to its mechanical superiority, design flexibility, enhanced safety, thermal, and chemical stability as compared to liquid electrolytes.[1–4] Polar polymers such as poly(vinylidene fluoride) (PVDF) and polyethylene oxide (PEO) are candidate materials for solid or gel electrolytes in secondary lithium-ion batteries. PVDF has strong electron-withdrawing groups along the backbones, and thus provides a high dielectric constant.[5–9] PEO provides effective ion conduction through the oxygen-ion interactions.[10–14] The crystallinity of PEO and PVDF are known to prohibit higher room-temperature ion conductivities in the solid state.[5–14] Blending of PEO and PVDF has been reported previously in order to reduce the crystallinity of both phases without introducing inactive components that are not beneficial to ion transport.[15–17] For example, Abraham et al.,[15] reported on a highly conductive polymer blend electrolyte with hexafluoropropylenecopymer of PVDF (known as PVDF-HFP), oligomeric poly(ethylene glycol) dimethyl ether ($CH_3O(CH_2-CH_2O)n$-CH_3, with average molecular weights $M_w = 250$, 400, and 500 g/mol, and lithium salts. Han et al.,[17] studied iodine ion transport in nanoparticle-modified PEO/PVDF blends in the context of a solid state redox electrolyte for dye-sensitized solar cells. In addition, several investigations of ion transport in PEO/(PVDF-HFP)/lithium perchlorate ($LiClO_4$) blends have been reported.[16,18,19] However, none provided detailed microstructure-performance relationships of the resultant blend electrolytes.

In the present work, we focus on establishing microstructure-performance relationships in a series of PEO/PVDF/lithium bis-(trifluoromethanesulfonyl) imide (LiTFSI)-based electrolytes

blends. LiTFSI is a benchmark salt for Li ion battery electrolytes. The PEO used in this study is synthesized by air-sensitive, anionic polymerization,[20] with a large molecular weight and small polydispersity (M_n = 270 kg/mol, PDI = 1.1) to eliminate effects from polymer chain sizes and distributions. A reciprocated suppression of polymer crystallization is identified at a PEO/PVDF ratio of 3:1 (by weight), and a detail microstructure characterization is carried out with electron and X-ray diffraction as well as energy filtered transmission electron microscopy (EF-TEM). The suppressed crystallization of both PEO and PVDF from PEO/PVDF/LiTFSI blends leads to a three-fold enhancement in room-temperature ion conductivities as compared to a control PEO/LiTFSI blend. The mechanical properties including elastic modulus (20–200 MPa) and hardness (1–20 MPa) of these blend electrolytes are highly tunable by simply varying blend compositions.

EXPERIMENTAL

Film Preparation

PEO is synthesized by anionic polymerization.[20] The molecular weight and polydispersity of the PEO polymer are well controlled and characterized (M_n = 270 kg/mol and PDI = 1.1). PVDF (M_w = 180 kg/mol, as received from Sigma Aldrich) is used without further treatment. LiTFSI is received from Sigma Aldrich and dried at 120 °C in inert-gas-filled glove box for 2 days before use. Proper amount of dry PEO, LiTFSI, and PVDF were weighted and dissolved in dimethylformamide (DMF), followed by subsequent thorough drying in a vacuum oven for 3 to 4 days at elevated temperatures (>100 °C). Samples were sealed in bags and stored in inert-gas-protected atmosphere before any subsequent testing and characterization.

Impedance Spectroscopy and Measurement

Conductivity was measured in the hermetically sealed coin cell via impedance spectroscopy (Solartron 1260 & 1286 combo) with voltage perturbation at 10 or 50 mV amplitude and frequency from 10 MHz to 0.1 Hz. In the cell, the polymer-LiTFSI disc sample (6.35 mm diameter and 0.8 mm thickness) prepared through hot pressing at elevated temperature (60 °C for PEO and 200 °C for the blended polymers) was sandwiched by two stainless steel spacers along with a 15 mil Teflon gasket under spring compression. Sample preparation and cell assembling were conducted in the Ar glove box and the cell was properly sealed with gasket and epoxy for the conductivity measurement in the ambient environment. Before measurement, the prepared cell was equilibrated at room temperature for a couple of days until the conductivity reached steady-state. The measurement temperature controlled by the close-top Teflon heating block started from 25 to 90 °C with 5 °C increment with 2 h of temperature equilibration prior to each measurement.

Thermal Properties

Differential scanning calorimetry (DSC) experiments were performed using TA instrument (Q1000) with a heat/cool/heat protocol under nitrogen flow. Samples were preheated to 250 °C to erase thermal and processing history, then cooled to −100 °C, and re-heated to 250 °C with a ramp rate of 10 °C/ min. The transition temperatures were determined by the first cooling and the second heating cycles.

Nanoindentation

Disc samples that were ∼1 mm thick were prepared from the solid blends and kept in airtight containers prior to test. Nanoindentation was performed on a TriboIndenter (Hysitron Inc.). A displacement control mode was used for experiments. For each sample, the peak penetration was fixed at 1000 nm, while the loading and unloading time were set at 5 s. At least 10 valid indentation data points were collected on each sample and the tests were completed within an hour. Elastic modulus and hardness values were calculated from the unloading curve according to the Oliver and Pharr method.[21]

X-Ray Diffraction

The solid blends were air-tight sealed in individual bags before experiments. X-ray diffraction (XRD) of the polymer electrolytes was then performed with a PanalyticalX'Pert using a copper K-alpha radiation.

Transmission Electron Microscopy

Dilute DMF solutions (0.2 wt %) of electrolytes were used to make drop-cast thin film on top of carbon coated copper grids. Transmission electron microscopy (TEM) experiments were conducted in a Zeiss Libra 120 with an Omega energy filter. A voltage of 120 kV and an emission current of about 5 μA were used in the experiments to minimize electron induced damage to electrolyte samples.

RESULT AND ANALYSIS

Figure 1(a) shows the temperature dependent ion conductivity for PEO/LiTFSI blends (containing 5 wt % LiTFSI) as a function of added PVDF concentration (0, 14, 25, and 50 wt %, in polymer matrix; e.g., a corresponding PVDF/PEO ratio of 0, 1/6, 1/3, and 1/1, by weight). A representative set of Cole–Cole plots of the electrolyte system are shown in Figure 1(b) as a function of PVDF loading at room temperature (25 °C). All electrolytes show an increase in conductivity at higher temperatures in the range of 25–90 °C. Blend electrolytes containing 14 and 50 wt % PVDF yield ion conductivities lower than PEO/LiTFSI system (0 wt % PVDF) in the measured temperature range (25–90 °C). Interestingly, the blend electrolyte containing 25 wt % PVDF significantly increases ion conductivity at lower temperature ranges (25–45 °C), by up to more than three-fold increase. For example, at 30 °C, the conductivity of the blend with 25 wt % PVDF is $1.5 \pm 0.1 \times 10^{-6}$ S/cm, while the conductivity of the blends with of 0 wt %, 14 wt %, and 50 wt % PVDF are $4.7 \pm 0.2 \times 10^{-7}$ S/cm, $2.7 \pm 0.1 \times 10^{-7}$ S/cm, and $1.3 \pm 0.1 \times 10^{-7}$ S/cm, respectively.

The conductivity of the blend electrolytes is associated with the changes in their microstructure and morphology at different temperatures. Therefore, we first examine thermal phase transitions including crystallization temperature (T_c) and melting temperature (T_m) by DSC. Figure 2 shows the first cooling (top data set) and the second heating cycles (bottom data sets) of the blend electrolytes. During cooling, the pristine

(a)

(b)
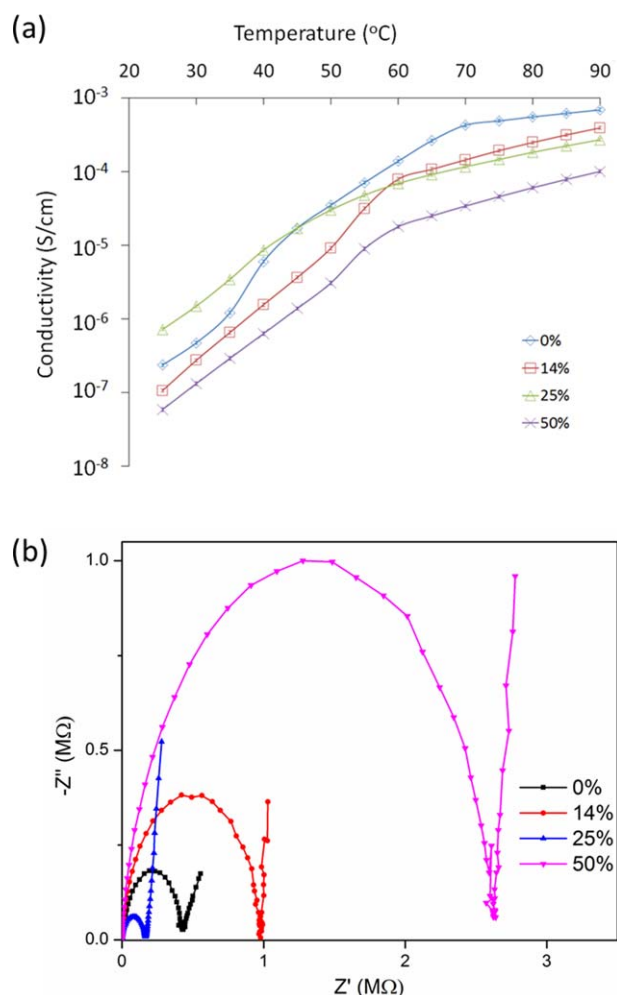
FIGURE 1 (a) Temperature-dependent ion conductivity of PEO-LiTFSI electrolytes (with 5 wt % LiTFSI) as a function of added PVDF (0, 14, 25, and 50 wt %). (b) Cole–Cole plots of PEO-LiTFSI (10:1) electrolytes as a function of added PVDF (0, 14, 25, and 50 wt %) at 25 °C. [Color figure can be viewed in the online issue, which is available at wileyonlinelibrary.com.]

PEO/LiTFSI system exhibits a large PEO crystallization ($T_c^{PEO} = 30$ °C). The crystallization of PEO is significantly suppressed by introducing PVDF 14, 25, and 50 wt % to the blends. It is also noted that the crystallization of PVDF appears at about 88 °C when adding relatively small amount of PVDF (14 and 25 wt %) and the T_c^{PVDF} further increase to 125 °C at higher PVDF composition (50 wt %).[22] In the second heating cycle, a characteristic T_m of PEO is observed at 54 °C in the PEO/LiTFSI sample, which is also greatly suppressed by PVDF additions. Melting peaks of PVDF (150–180 °C) become pronounced with higher PVDF composition in the blends. Evidently, 14–25 wt % of PVDF provides a reciprocated suppression of both PEO and PVDF crystallizations. This is featured not only by the large reduction of PEO and PVDF transition peak intensities (including melting and crystallization), but also through the decreased crystallization and melting temperatures of PVDF. In addition, looking back at the conductivity measurements, we noticed a distinctive slope change at

40–60 °C in temperature-dependent conductivities for all samples, which correlates to PEO crystallite melting. The semi-crystalline electrolyte systems are able to improve their ion conductivity by more than three orders of magnitudes upon the transition to a largely amorphous state.

Interestingly, the blend electrolytes do not exhibit distinct melting or crystallization peaks of PEO under current DSC measurement conditions which indicates crystallization of PEO is significantly suppressed by the presence of PVDF crystallites. Meanwhile, crystallinity of PVDF for PEO/PVDF blends is determined by using the equation of $X_c = \Delta H_f / \Delta H_f^*$ $\times$ 100%, where ΔH_f is the enthalpy of fusion from DSC measurement and ΔH_f^* is the enthalpy of fusion of 100% crystalline PVDF (104.7 J/g).[23] The X_c values of PVDF are found to be 5.1, 11.2, and 25.2% for blend electrolytes containing 14, 25 and 50 wt % PVDF, respectively (Table 1).

Crystallinity is one of the most important factors that determines ion conductivity at room temperature and can be reflected by its mechanical properties. The mechanical properties of PEO-LiTFSI blends upon PVDF addition are herein examined by nanoindentation. Both elastic modulus and hardness of the composite electrolyte films are extracted and compared in Figure 3. The addition of PVDF is found to reduce the elastic modulus and hardness of the systems when the ratio of PVDF increases from 0 to 14 wt %. As the PVDF concentration increases further from 14 to 50 wt %, both elastic modulus and hardness of the blends increases. The elastic modulus and hardness of the pristine PEO-LiTFSI systems are 140 ± 10 MPa and 5.3 ± 0.3 MPa, respectively. The addition of 14 wt % PVDF reduces these values to 20 ± 2 MPa and 1.2 ± 0.2 MPa. At 25 wt % PVDF, the elastic modulus and hardness of the blends increase back to
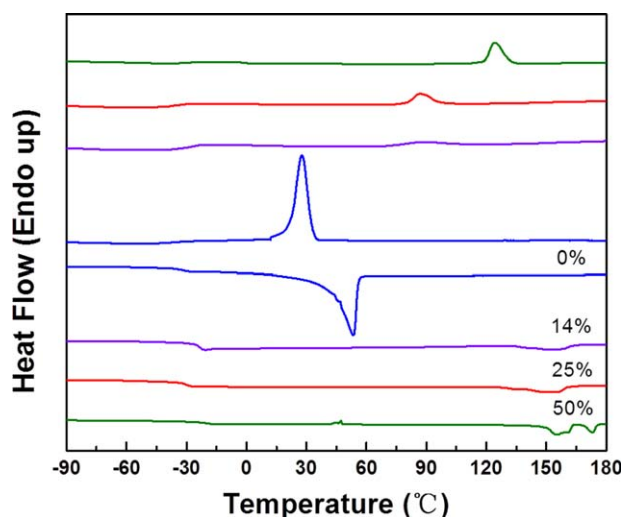
FIGURE 2 The first cooling (top data set) and second heating DSC scans (bottom data set) of PEO/LiTFSI (5 wt % LiTFSI) blends as a function of added PVDF content. [Color figure can be viewed in the online issue, which is available at wileyonlinelibrary.com.]

TABLE 1 Enthalpy and Crystallinity of Blend Electrolytes

Blend Electrolytes	ΔH_f (J/g)[a]	X_c (%)[b]
0 wt % PVDF	89.5[c]	41.9[c]
14 wt % PVDF	5.3	5.1
25 wt % PVDF	11.7	11.2
50 wt % PVDF	26.4	25.2

[a] Determined from the second heating of DSC measurement.
[b] Determined by $X_c = \Delta H_f/\Delta H_f^* \times 100\%$, where ΔH_f^* is the enthalpy of fusion of 100% crystalline PVDF (104.7 J/g) and PEO (213.7 J/g).[24]
[c] These values are associated with PEO crystals, whereas the rest of values relate to PVDF crystals.

110 ± 3 MPa and 7.6 ± 1.1 MPa. Finally, at 50 wt % PVDF, the elastic modulus and hardness are all enhanced to the highest values of to 200 ± 10 MPa and 20.3 ± 1.3 MPa, respectively. The measured modulus of PEO without PVDF addition at room temperature is comparable to the values previously reported by Cimmino et al.[25] This nonlinear dependence of mechanical properties on PVDF concentration can be attributed to the reciprocated suppression of PEO and PVDF crystallization observed in DSC. The large reduction of PEO crystallization in the presence of a small amount of PVDF (less than 14 wt %) is mainly responsible for decreasing mechanical properties at lower PVDF concentrations, while the higher PVDF concentration (greater than 14 wt %) leads to increased PVDF crystallization and thus enhanced mechanical properties.

To further examine the microstructure evolution of PVDF-PEO-LiTFSI blends, X-ray diffraction results were carried out as shown in Figure 4(a). The X-ray diffraction peaks from pristine PEO-LiTFSI electrolyte can be divided into two groups: (1) peaks from pristine PEO and (2) peaks from P(EO)$_6$LiTFSI salt-polymer complex, which is consist-
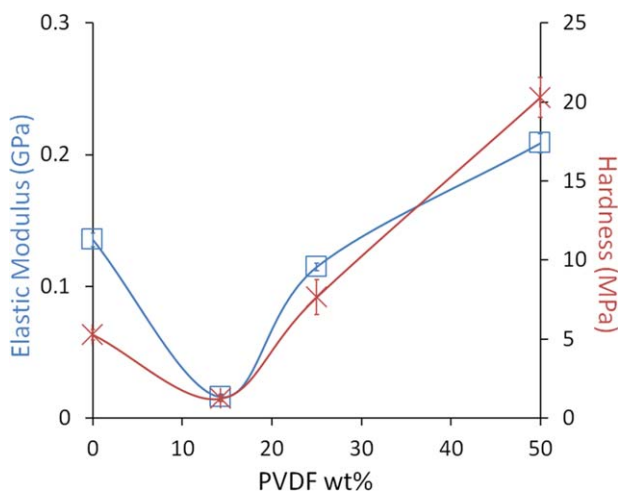
FIGURE 3 Elastic modulus and hardness of PEO-LiTFSI (5 wt % LiTFSI) electrolytes as a function of added PVDF weight percentage (0, 14, 25, and 50 wt %) as determined by nanoindentation experiments. [Color figure can be viewed in the online issue, which is available at wileyonlinelibrary.com.]

ent with previous reports.[10,11,14,26] These peaks are largely eliminated at 14–50 wt % PVDF loadings, when reflections from PVDF crystallites gradually appear. The (100) and (020) peaks of PVDF increase significantly when the PVDF loading reaches 50 wt %. These data provide further evidences regarding the reciprocated suppression of crystallization in PVDF and PEO matrix.

Using Gaussian functions for XRD fitting and Scherrer equation,[28] efforts were made to correlate crystal sizes and XRD peak intensities with PVDF loading level. The Scherrer equation takes the form of

$$L = \frac{K\lambda}{\beta \cos \theta}, \qquad (1)$$

where L stands for a average size of crystallites, θ for the Bragg angle, K for dimensionless shape factor, β for the line broadening at Full Width Half Maximum (FWHM), and λ for the wavelength of incident X-ray beam. In the calculation, constant value of $K = 0.9$ and $\lambda = 1.5406$ Å are used. The PVDF loading dependent XRD peak intensity and crystal dimension are available in Table 2 and illustrated in Figure 4(b–e) for PVDF (020) and PEO peak of $2\theta = 14.8°$. Significant crystallinity of PEO suppression was observed with addition of PVDF. Both peak intensity and crystal dimension of PEO dramatically drop when PVDF is added, while at the same time, those of PVDF clearly increase.

In Figure 5, selected area electron diffraction (SAED) patterns of the blend electrolyte systems also suggest a strong PVDF percentage dependence, in agreement with the X-ray diffraction results in Figure 4. The pristine PEO/LiTFSI sample has distinctive sharp reflections, such as ($\bar{2}$24) from PEO crystals, based on the reported monoclinic PEO unit cell.[29,30] These PEO reflections disappear at PVDF concentrations of 14–50 wt %. In addition, the PVDF (020) diffraction ring becomes rather distinctive at 50 wt % PVDF loading, which indicates that the PVDF crystalline packing at 50 wt % of PVDF is considerably more regular as compared to those in other compositions.

Energy filtered TEM of PVDF-PEO-LiTFSI blends are further conducted to reveal the detailed phase separations responsible for the observed mechanical and electrical properties. Figure 6 shows the 0 eV images (elastic, top row) and composite oxygen (red) + fluorine (green) maps (bottom row), for blends with 0, 25 wt %, and 50 wt % PVDF. The non-homogeneous, localized oxygen- or fluorine- rich domains, on the order of 50–100 nm are distinctive in the pristine PEO-LiTFSI system, which are attributed to aggregated pristine PEO and P(EO)$_6$LiTFSI salt complex components. These aggregated domains mostly disappear in the blend with 25 wt % PVDF, which exhibit well dispersed components with uniform oxygen and fluorine distributions. It should be noted that in the blends with added PVDF, oxygen can originate from PEO or the P(EO)$_6$LiTFSI complex, while fluorine can originate from either LiTFSI or PVDF (in the pristine PEO/LiTFSI blend, fluorine should only originate from LiTFSI.) At
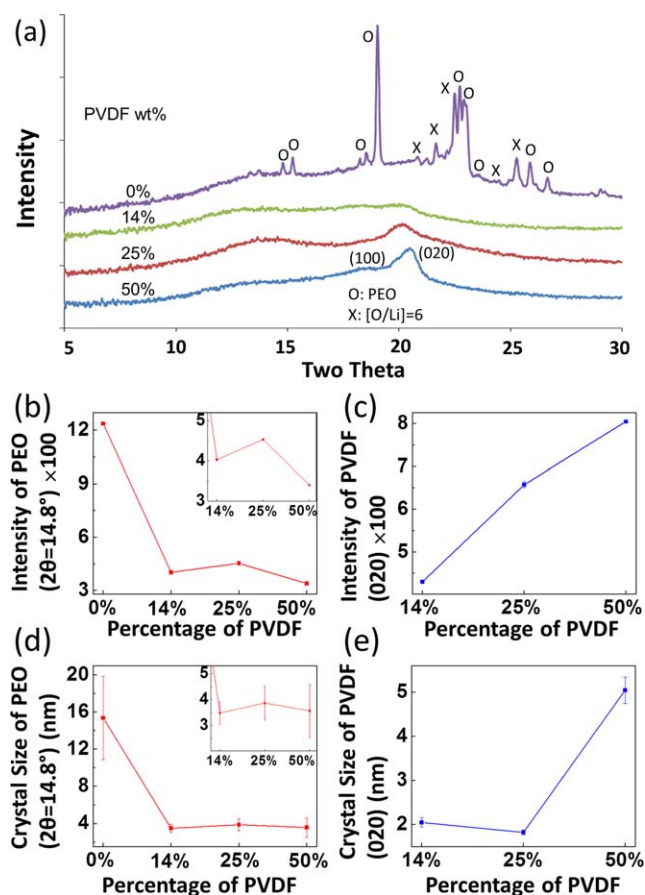
FIGURE 4 (a) X-ray diffraction of PEO-LiTFSI (5 wt % LiTFSI) electrolytes as a function of added PVDF weight percentage (0, 14, 25, and 50 wt %). The peaks from pristine PEO are labeled with circles "O," and the peaks from the $(PEO)_6$:LiTFSI complex are marked with crosses "X." The reflections from PVDF are labeled with their Miller indices. The PVDF loading dependent XRD peak intensity in PVDF/PEO/LiTFSI electrolytes for (b) PEO peak of $2\theta = 14.8°$ and (c) PVDF (020). The PVDF loading dependent crystal dimension in PVDF/PEO/LiTFSI electrolytes for (d) PEO peak of $2\theta = 14.8°$ and (e) PVDF (020). [Color figure can be viewed in the online issue, which is available at wileyonlinelibrary.com.]

50 wt % PVDF, clusters with aggregated oxygen- and fluorine- rich domains have sizes greater than 200 nm (Fig. 6). We attribute this mainly to the PVDF-PEO phase separation because LiTFSI does not have its separated domains as evidenced by SAED, DSC, and XRD.

The schematics shown in Figure 7 summarize the key findings of the microstructure characterizations from this work in a simplified format. With no PVDF added, PEO and LiTFSI have a locally concentrated distribution (or phase separation) due to PEO crystallization and crystalline complex formation of $P(EO)_6LiTFSI$. When 25 wt % PVDF was introduced into the blend, a less heterogeneous, highly conductive system forms because of the reciprocated suppression of both PEO and PVDF crystallization. With further elevated PVDF loading, a separated PVDF crystalline phase comes into formation, which deteriorates the ion conductivity.

DISCUSSION

The reciprocated suppression of polymer crystallization is valuable for several reasons. (1) Both polymer components in the matrix can contribute toward effective ion transport. In our case, the local dipole moments in both PEO and PVDF are critical to their ion conductivities, which are distinctively different than the concept of inert additives. The use of inert additives such as oxide nanoparticles can also lead to performance enhancement, however, the inert additives will not conduct ions by themselves, and solely rely on their interactions with their matrix, or the changes they induce in the matrix. (2) Both polymer components require suppression of crystallization to achieve more efficient ion transport. The amorphous regions of PEO are known to contribute largely to their high conductivity,[10–14] while PVDF performs well in the gel-like format.[5–9] (3) The coordination between PEO and PVDF crystallite suppression at a proper blend ratio provides a possibility to harvest the best performance from both polymer components simultaneously.

Previous studies on PVDF and PEO blending are very limited.[14–18] The hexafluoropropylene copolymers of PVDF (PVDF-HFP) were reported to blend with $LiClO_4$ and PEO polymer in electrolyte applications.[15,17,18] The $LiClO_4$ as a salt was often used in earlier studies (for example, in 1980's), which was not active in wide applications any more. In addition, processing conditions and electrolyte performance were the main focus of these works, while the detailed structure-performance correlations were not provided. In another previous study, PVDF-HFP copolymers and oligomer versions of PEO (degree of polymerization DP = 10, 8, and 5) were blended with lithium salts to improve conductivity. The amorphous, gel or liquid-like nature of the oligomer PEOs in this study indicated that there was no reciprocated suppression of

TABLE 2 Peak Intensity and Crystal Dimension of PEO and PVDF Separately

Blend Electrolytes	Intensity of PEO (2 = 14.8°)	Intensity of PVDF	Dimension (nm) of PEO Crystallite (2 = 14.8°)	Dimension (nm) of PVDF Crystallite
0 wt % PVDF	1237 ± 0.71	0	15.4 ± 4.48	0
14 wt % PVDF	402 ± 2.92	430 ± 1.39	3.48 ± 0.43	2.05 ± 0.11
25 wt % PVDF	453 ± 2.40	657 ± 6.94	3.86 ± 0.65	1.82 ± 0.06
50 wt % PVDF	340 ± 1.21	805 ± 3.51	3.56 ± 1.04	5.04 ± 0.30
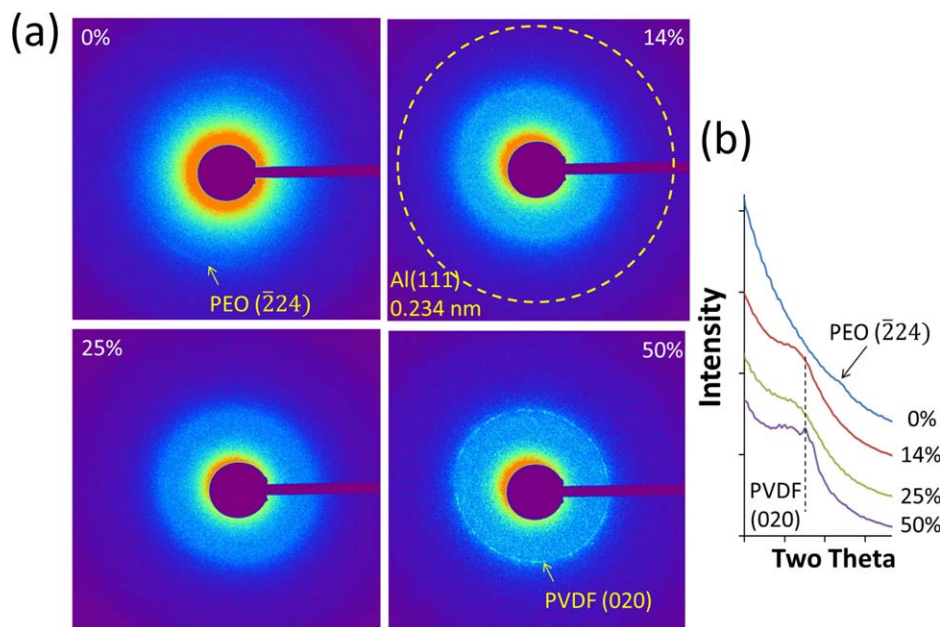
FIGURE 5 (a) Selected area electron diffraction pattern of PEO-LiTFSI (5 wt % LiTFSI) blends as a function of the added PVDF concentration. (b) One-dimensional azimuthally averaged radial profiles are given on the right. [Color figure can be viewed in the online issue, which is available at wileyonlinelibrary.com.]

crystallization involved and there was only one crystalline polymer in the matrix (PVDF-HFP). In the present case, because of the binary polymer matrix and reciprocated sup-

pression of polymer crystallization, a new opportunity of performance tuning is opened up for both ion conductivity and mechanical properties.
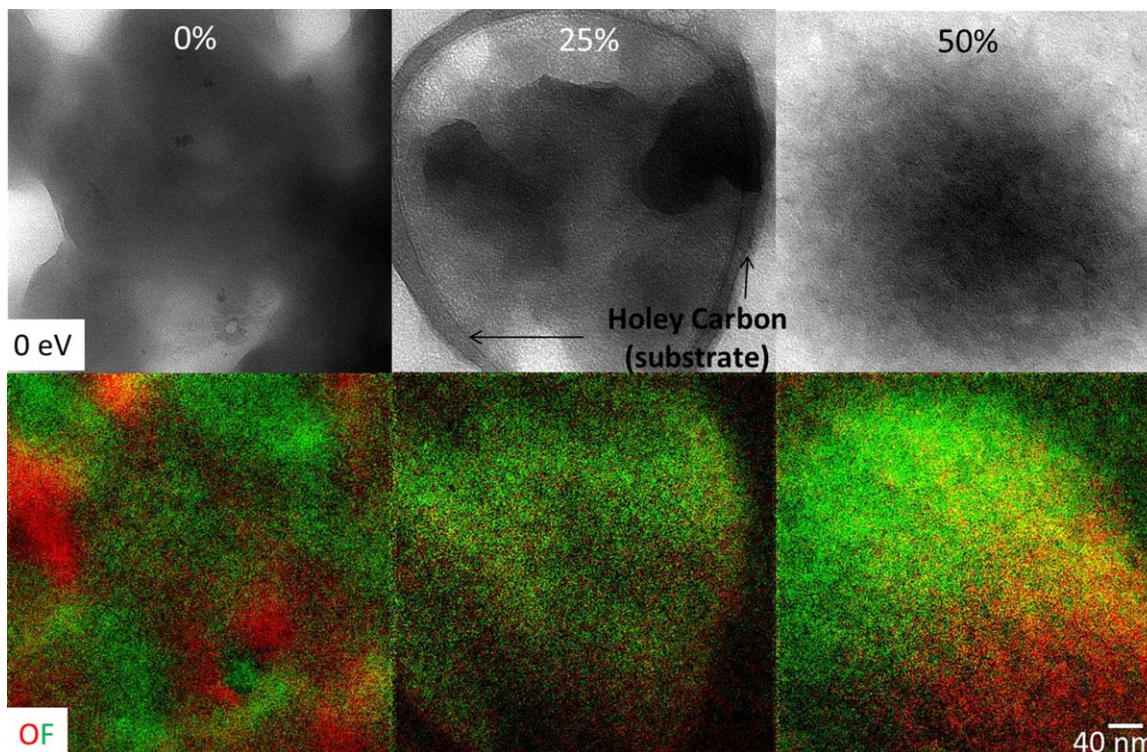
FIGURE 6 Energy filter TEM images of PEO-LiTFSI (10:1) electrolytes as a function of added PVDF weight percentage (0, 25, and 50 wt %). Elastic images are shown in the top row, and the corresponding composite images (Oxygen in red and Fluorine in green) are in the bottom row. [Color figure can be viewed in the online issue, which is available at wileyonlinelibrary.com.]
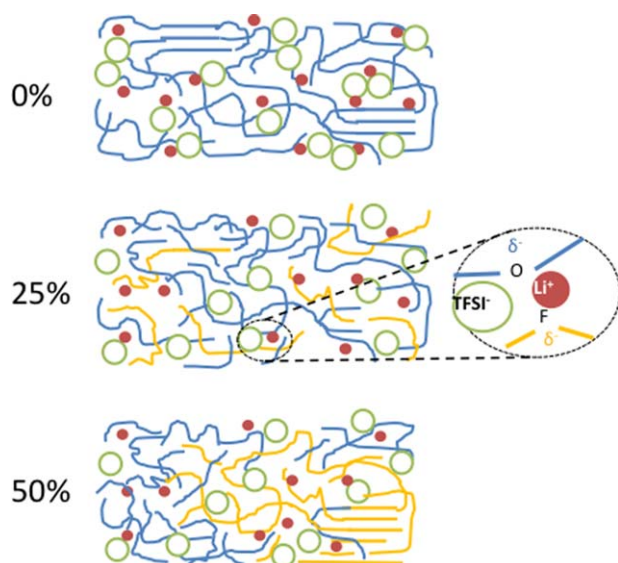
FIGURE 7 Schematics showing the proposed structures of PEO/LiTFSI electrolytes as a function of PVDF concentration. Red dots and green circles represent Li^+ and TFSI-, respectively. Blue lines represent PEO while yellow lines serve as PVDF. [Color figure can be viewed in the online issue, which is available at wileyonlinelibrary.com.]

Nanoparticle fillers are know to provide an alternative approach toward PEO crystallinity suppression and performance enhancement. One may argue that the functions of PVDF may be partially replaced by nanoparticles in lithium conducting PEO electrolytes. However, the nanoparticles used so far are mostly made up of metal oxides, which are inert in terms of lithium conducting. Nanoparticle aggregation and dispersion impose additional challenges and complications. A 10% wt nanoparticle loading typically correlates with highest-possibly-achieved ion conductivity, which provides very limited property tuning windows. On the other hand, the reciprocated suppression of polymer matrix crystallization offers a possible route toward an electrolyte system with no inert, non-conducting component and wide range of property tunabilities, free of nanoparticle aggregation issues.

Based on our findings, the PEO and PVDF crystallite suppressions have a rather intriguing synergistic effect. Previous work on a complex PEO/PVDF/Iodine ion/nanoparticle system reported an optimal blend ratio of 6:4 (by weight) in generating ideally reciprocated suppression.[17] This is considerably different from our optimal ratio of 3:1 (PEO/PVDF by weight). Their nanoparticle loading can complicate this comparison, along with their different choice of salt. The asymmetrical 3:1 ratio that was optimized in the present work can be attributed to the polarity differences of PEO and PVDF, which translate into their tendencies (or free energy reduction) to crystallize at room temperature. The highly polar PVDF has a stronger tendency to pack in crystalline lattice at room temperature, so that the best performing

PVDF electrolytes are typically gel-like. In comparison, PEO is less polar, and can be optimized as solid-state electrolyte.

Interestingly, it is noticed that the highest room temperature conductivity occur at 25% wt PVDF loading (Fig. 1), while the lowest mechanical properties occurs at 14% wt PVDF loading (Fig. 3). We believe the subtle balance between PEO and PVDF crystallinity and crystallite size distributions upon the reciprocated suppression likely leads to this intriguing effect. With only 14% wt PVDF, the weak PVDF crystallinity and their relatively small sizes play a main role in achieving the lowest elastic modulus and hardness, because of the higher intendancy for PVDF molecules to pack up in lattice and crystallize. With 25% wt PVDF, however, the weaker PEO crystallinity and their size distributions optimize room temperature ion conductivity, while the increased PVDF crystallinity and packing enhance the mechanical properties of the resultant composite electrolyte.

This work has thus laid the foundation for establishing structure-property correlations and reciprocated suppression of polymer crystallization for solid-state electrolytes. We pursued a comprehensive approach to correlate indirect and direct microstructural characterization, with both diffraction techniques and energy filtered TEM. A correlation between mechanical and electrical properties was performed to understand the underlying microstructural evolution as a function of blend composition. Future developments of the reciprocated suppression of polymer crystallization can be made through several mechanisms: (1) Molecular weight and polydispersity of the individual polymer components can be varied toward ion transport optimization. (2) Copolymer or interfacial compatibilizers can be synthesized and used in the binary polymer interface or as the sole polymer matrix. This will lead to confined nanophase separation between the two active polymer components, and can further suppress the crystallization of the two polar polymer matrices. (3) Incorporation of newer-generation, high-performance salts can be also crucially beneficial. Chemical bonding between salt and the individual polymer components is expected to have more effective reciprocated suppression of the two polar polymer components and provide more tunability for mechanical properties and room-temperature ion conductivities.

CONCLUSIONS

In summary, we investigated the reciprocated suppression of PVDF and PEO crystallization as well as structure-electrical/ mechanical property relationships in PEO/PVDF/LiTFSI-based electrolytes. With electron and X-ray diffraction combined with energy filtered transmission electron microscopy (EF-TEM), we identify and examine the optimal blending range that is responsible for diminishing of both PVDF and PEO crystallites. A three-fold conductivity enhancement is herein achieved, along with a highly tunable elastic modulus (20–200 MPa), which is expected to contribute toward future designs of solid polymer electrolytes with high room-temperature ion conductivities and mechanical flexibility.

ACKNOWLEDGMENTS

REFERENCES AND NOTES

1 J. M. Tarascon, M. Armand, *Nature* **2001**, *414*, 359–367.

2 D. T. Hallinan Jr., N. P. Balsara, *Annu. Rev. Mater. Res.* **2013**, *43*, 503-+.

3 A. M. Stephan, K. S. Nahm, *Polymer* **2006**, *47*, 5952–5964.

4 C.-N. Sun, T. A. Zawodzinski, W. E. Tenhaeff, F. Ren, J. K. Keum, S. Bi, D. Li, S.-K. Ahn, K. Hong, A. J. Rondinone, J.-M. Y. Carrillo, C. Do, B. G. Sumpter, J. Chen, *Phys. Chem. Chem. Phys.* **2015**, *17*, 8266–8275.

5 Z. Jiang, B. Carroll, K. M. Abraham, *Electrochim. Acta* **1997**, *42*, 2667–2677.

6 K. M. Kim, K. S. Ryu, S. G. Kang, S. H. Chang, I. J. Chung, *Macromol. Chem. Phys.* **2001**, *202*, 866–872.

7 D. Saikia, A. Kumar, *Electrochim. Acta* **2004**, *49*, 2581–2589.

8 S. Ramesh, S.-C. Lu, *J. Mol. Struct.* **2011**, *994*, 403–409.

9 S. Abbrent, J. Plestil, D. Hlavata, J. Lindgren, J. Tegenfeldt, A. Wendsjo, *Polymer* **2001**, *42*, 1407–1416.

10 S. Lascaud, M. Perrier, A. Vallee, S. Besner, J. Prudhomme, M. Armand, *Macromolecules* **1994**, *27*, 7469–7477.

11 A. Vallee, S. Besner, J. Prudhomme, *Electrochim. Acta* **1992**, *37*, 1579–1583.

12 W. Gorecki, M. Jeannin, E. Belorizky, C. Roux, M. Armand, *J. Phys.-Condens. Matter* **1995**, *7*, 6823–6832.

13 R. C. Agrawal, G. P. Pandey, *J. Phys. D-Appl. Phys.* **2008**, 41

14 M. Marzantowicz, J. R. Dygas, F. Krok, J. L. Nowinski, A. Tomaszewska, Z. Florjanczyk, E. Zygadlo-Monikowska, *J. Power Sources* **2006**, *159*, 420–430.

15 K. M. Abraham, Z. Jiang, B. Carroll, *Chem. Mater.* **1997**, *9*, 1978–1988.

16 M. M. E. Jacob, S. R. S. Prabaharan, S. Radhakrishna, *Solid State Ionics* **1997**, *104*, 267–276.

17 H. W. Han, W. Liu, J. Zhang, X. Z. Zhao, *Adv. Funct. Mater.* **2005**, *15*, 1940–1944.

18 M. Deka, A. Kumar, *Bull. Mater. Sci.* **2009**, *32*, 627–632.

19 L. Z. Fan, Z. M. Dang, C. W. Nan, M. Li, *Electrochim. Acta* **2002**, *48*, 205–209.

20 D. Uhrig, J. W. Mays, *J. Polym. Sci. Part A: Polym. Chem.*, **2005**, *43*, 6179–6222.

21 W. C. Oliver, G. M. Pharr, *J. Mater. Res.* **1992**, *7*, 1564–1583.

22 D. R. Dillon, K. K. Tenneti, C. Y. Li, F. K. Ko, I. Sics, B. S. Hsiao, *Polymer* **2006**, *47*, 1678–1688.

23 Y. D. Wang, M. Cakmak, *J. Appl. Polym. Sci.* **1998**, *68*, 909–926.

24 K. Prabakaran, S. Mohanty, S. K. Nayak, *RSC Adv.* **2015**, *5*, 40491–40504.

25 S. Cimmino, E. Martuscelli, L. Nicolais, C. Silvestre, *Polymer* **1978**, *19*, 1222–1223.

26 M. Marzantowicz, J. R. Dygas, F. Krok, A. Lasinska, Z. Florjanczyk, E. Zygadlo-Monikowska, A. Affek, *Electrochim. Acta* **2005**, *50*, 3969–3977.

27 F. Wu, T. Feng, Y. Bai, C. Wu, L. Ye, Z. Feng, *Solid State Ionics* **2009**, *180*, 677–680.

28 A. L. Patterson, *Phys. Rev.* **1939**, *56*, 978–982.

29 Y. Takahash, H. Tadokoro, *Macromolecules* **1973**, *6*, 672–675.

30 M.-S. Hsiao, W. Y. Chen, J. X. Zheng, R. M. Van Horn, R. P. Quirk, D. A. Ivanov, E. L. Thomas, B. Lotz, S. Z. D. Cheng, *Macromolecules* **2008**, *41*, 4794–4801.